



1 **Gasoline aromatic: a critical determinant of urban secondary organic aerosol formation**

2

3 Jianfei Peng^{1,†}, Min Hu^{1,4*}, Zhuofei Du¹, Yinhui Wang², Jing Zheng¹, Wenbin Zhang², Yudong Yang¹,
4 Yanhong Qin¹, Rong Zheng², Yao Xiao¹, Yusheng Wu¹, Sihua Lu¹, Zhijun Wu¹, Song Guo¹, Hongjun
5 Mao³, Shijin Shuai^{2,*}

6

7 ¹ State Key Joint Laboratory of Environmental Simulation and Pollution Control, College of
8 Environmental Sciences and Engineering, Peking University, Beijing 100871, China

9 ² State Key Laboratory of Automotive Safety and Energy, Tsinghua University, Beijing 100084, China

10 ³ College of Environmental Sciences and Engineering, Nankai University, Tianjin 300071, China

11 ⁴ Beijing Innovation Center for Engineering Science and Advanced Technology, Peking University

12 [†] Now at Department of Atmospheric Sciences, Texas A&M University, College Station, TX 77843,
13 US

14 *Corresponding author: Min Hu, minhu@pku.edu.cn; Shijin Shuai, sjshuai@tsinghua.edu.cn

15 **Abstract**

16 Gasoline vehicle exhaust is an important contributor to secondary organic aerosol (SOA) formation in
17 urban atmosphere. Fuel composition has considerable potential impact on gasoline SOA production, but
18 this impact is still taken little account in the emission regulations due to the poor understanding of the
19 link between fuel components and SOA production. Here, we present an in-depth study to investigate
20 the impact of gasoline aromatic content on SOA production through chamber approach. A significant
21 amplification factor of 3 - 6 for SOA productions from gasoline exhausts was observed as gasoline
22 aromatic content rose from 29% to 37%. Considerably higher emissions of both monocycle and
23 polycyclic aromatic volatile organic compounds performed an essential role in the SOA production
24 enhancement. Our findings indicate that gasoline aromatics have significant influence on ambient PM_{2.5}
25 concentration in megacities and highlight that more stringent regulation on gasoline aromatic content
26 will achieve unexpected benefit on air quality in urban areas.

27

28 **1 Introduction**

29 Fossil fuel-powered vehicles, an important source of NO_x, volatile organic compounds (VOCs)
30 and atmospheric particulate matter (PM), are always associated with the severe haze events, human
31 health risks and climate forcing, particularly in urban areas (Guo et al., 2014;Huang et al., 2014;Parrish
32 and Zhu, 2009;Kumar et al., 2014;Peng et al., 2016b;Kelly and Zhu, 2016;Liu et al., 2015a). Gasoline is
33 the most widely used vehicle fuel and accounts for the largest total transportation energy consumptions



34 in many countries (NBSC, 2015; EIA, 2015), e.g., U.S. and China. Among all the gasoline PM
35 components, secondary organic aerosols (SOA) produced via atmospheric oxidation of VOC precursors
36 in the exhaust have been proved by chamber experiments as a large fraction, if not the largest, of gasoline
37 vehicular PM (Platt et al., 2014; Liu et al., 2015b; Gordon et al., 2014a; Jathar et al., 2014; Zervas et al.,
38 1999; Jimenez et al., 2009). Moreover, ambient measurement also demonstrated that gasoline SOA were
39 the largest source of vehicular carbonaceous PM in megacities such as Los Angeles (Bahreini et al.,
40 2012). However, though increasingly stringent gasoline fuel standards, especially on sulfur content, have
41 been implemented in the past decades in many countries to reduce the exhaust emissions, current gasoline
42 fuel standards don't take enough account to the SOA production. This contradiction is mainly attributable
43 to the poor understanding of the effects of fuel properties on the related SOA formation, and may
44 ultimately lead to a policy bias on the control of vehicle emission regarding to the reduction of
45 atmospheric pollution.

46 Aromatic hydrocarbons, unsaturated compounds with at least one benzene ring-like structure,
47 account for 20% - 40% v/v of gasoline fuel. Aromatic VOCs (i.e., toluene, xylenes and trimethylbenzenes)
48 react exclusively with the OH radical in the atmosphere, leading to the formation of a variety of low
49 volatile species (e.g., benzoic acid) (Zhang et al., 2015), which will partition onto existing particle and
50 be recognized as anthropogenic SOA. Therefore, the higher emission of aromatic VOCs will likely result
51 in more SOA formation potential. Existing fuel-effect experimental and model studies have exhibited
52 that high-aromatic fuel in gasoline fuel will lead to more emissions of primary PM as well as some
53 aromatic VOCs (Karavalakis et al., 2015; Yinhuai et al., 2016; Zervas et al., 1999; Agency, 2013),
54 indicating the considerable potential impact of gasoline aromatic content on SOA production.
55 Furthermore, though aromatic content in diesel fuel may have little impact on SOA formation (Gordon
56 et al., 2014b), SOA production from gasoline vehicle is considered to be more sensitive to aromatic
57 content than that from diesel vehicle (Jathar et al., 2013). However, till now, very few studies have
58 successfully quantified the impact of gasoline aromatic content on SOA production and directly revealed
59 the possible pathway.

60 In this study, an in-depth comprehensive research was conducted to investigate the link between
61 gasoline fuel compositions, primary gas- and particle- phase emission, and corresponding SOA formation.
62 Gasoline exhaust emissions were examined on two platforms under two different conditions. The first
63 platform was the chassis dynamometer system equipped with a constant volume sampler (CVS). Vehicle



64 exhausts after CVS was introduced into an outdoor environmental chamber and underwent aging under
65 typical polluted urban condition to simulate the SOA formation in ambient atmosphere. The second
66 platform was the experimental engine system on which emissions from a port gasoline injection (PFI)
67 engine and a gasoline direct injection (GDI) engine were examined. SOA formation experiments from
68 engine exhausts were carried out under strong oxidizability condition to obtain the highest SOA
69 production potential. Most importantly, different gasoline fuels blended from different refinery streams
70 were utilized in both platforms to probe the critical link among fuel components, VOCs emissions and
71 related SOA production.

72 **2 Materials and methods**

73 **2.1 Test fleet, cycle and engine.**

74 In order to explore the SOA formation from gasoline vehicles with different standard stage and
75 different working situation, both vehicle dynamometer PFI and PFI engine emission were tested in this
76 work.

77 The chosen PFI vehicle belonged to a commonly used vehicle model in China, which certified to
78 China IV emission standard (equivalent to Euro 4). The mileage of the test fleet was about 3000 km. The
79 fleet was driven on a chassis dynamometer system (Burke E. Porter Machinery Company) using cold-
80 start Beijing cycle in order to better simulate the actual driving situation in Beijing. Beijing cycle was
81 about 17 min long, with highest speed about 50 km (Fig. S1). The temperature and the absolute humidity
82 in the dynamometer room were kept at $23.0 \pm 1.0^\circ\text{C}$ and $8.4 \pm 0.9\text{ g m}^{-3}$, respectively, for all vehicle
83 experiments (Table S1).

84 Vehicle exhaust underwent the first stage of dilution with filtered ambient air using a constant
85 volume sampler (CVS) operated at $5.5\text{ m}^3\text{ min}^{-1}$ for all experiments. Approximately 5.3 L min^{-1} of diluted
86 exhaust from the CVS was introduced into the 1.2 m^3 chamber to be further diluted with the clean air in
87 the chamber (Fig. 1). The average dilution factor was approximately 20 in the CVS and was
88 approximately 15 in the chamber. During the entire cycle, a light-duty gasoline vehicle emissions testing
89 system (HORIBA, Ltd.) was used to measure the average and real-time concentration of THC, CO_2 , CO,
90 CO_2 and NO_x .

91 The PFI and GDI engines were manufactured by a domestic Chinese automaker and equipped with
92 turbocharger together with downsized displacement. The operation mode of the PFI engine for chamber



93 experiments was 2000 round per minute with 50% loading. After the engine became stable at this
94 operating mode, the exhaust were introduced into the chamber passing through a heater (150° C) and a
95 filter, with a flowrate of 5 L/min for 1 min. During the injection, the emission was transferred from the
96 engine exhaust system into the chamber, successively. Particle number, mass and chemical composition,
97 as well as VOCs in the exhaust were characterized at the same operating mode. Detail description of the
98 engine experiments can be found in our previous study (Du et al., 2017) and all engine experiments used
99 in this study are illustrated in Table S2.

100 **2.2 Fuels**

101 Three fuels (F1, F2 and F3) were utilized in this study to investigate the impacts of the gasoline
102 fuel on SOA formation. A commercial Phase V gasoline (F1 fuel) with equivalent octane number of 93
103 was used as the base fuel. F1 fuel contains 30% aromatics and 4% olefin content (Table S3).

104 F2 fuel was blended from 80% of F6 fuel and 20% of refinery catalytic stream. Octane level and
105 aromatic content (28.5%) in F2 fuel are very similar with that in F1 fuel, with the only difference to be
106 the olefin content.

107 F3 fuel was blended from 80% of F2 fuel, 15–20% of refinery reformate stream and very small
108 amount of o-octane and n-heptane to keep the same octane level. Compared with F2 fuel, F3 fuel contains
109 similar olefin content (15%) but higher aromatic content (37%) (Table S3), but both F2 and F3 fuels
110 meet the Phase V gasoline standard. Detail information about the fuels can be found in our previous
111 paper (Yinhui et al., 2016).

112 On the basis of the aromatic contents, the F2 and F3 fuel can be well representative of the fuel
113 normally used in the year around 2010 and after 2013 in Chinese market such as Beijing and Shanghai,
114 respectively.

115 **2.3 Chamber Simulation**

116 The quasi-atmospheric aerosol evolution study (QUALITY) chamber was utilized were conducted
117 to quantify SOA formation from both gasoline engine exhaust and gasoline vehicle exhaust. The 1.2 m³
118 two-layer chamber was comprised of an inner layer of 0.13 mm PFA Teflon and an outer rigid 5.6 mm
119 thick acrylic shell (Cryo Industries Acrylite, OP-4). Both of them allowed for efficient transmission of
120 sunlight in UV ranges (Peng et al., 2016b). Pre-experiments have shown that wall loss decreased the
121 particle number concentration by about 50% in about 2-3 hours, SO₂ and NO_x decreased to about 50%



122 after 20 hours, while toluene and isoprene did not show obvious wall loss during a two-day experiment
123 (Peng et al., 2016b).

124 Prior to each experiment, the QUALITY chamber was covered with two layers of anti-UV cloth to
125 shield the chamber from sunlight and flushed by zero air for more than 15 hours to ensure a clean
126 condition. In both vehicle and engine experiments, excess (1 ml 30%) H₂O₂ was also injected into the
127 chamber via the makeup air flow as an extra hydroxyl radical (OH) source after adding the exhaust to
128 perform. Chamber experiments were mainly conducted from noon to later afternoon, with inside
129 temperature of 30 - 35 °C and of relative humidity (RH) of 40 - 60%. A suite of high time resolution
130 state-of-the-art aerosol instruments were utilized to simultaneously measure the gas concentration and a
131 comprehensive set of particle properties throughout the experiments, including concentrations of HONO,
132 SO₂, NO_x, O₃, CO, CO₂ and several VOCs, the particle diameter, mass, chemical composition (Fig. 1).

133 During each chamber experiment, a suite of state-of-art instruments was utilized to characterize
134 the evolution of gas- and particulate- phase pollutants intermittently (Table S4). Particle number
135 distributions were measured with a scanning mobility particle sizer (SMPS) system, which was
136 composed by one differential mobility analyzer (DMA, TSI, Inc., model 3081) and one condensation
137 particle counter (CPC, TSI, Inc., model 3772). The mass concentration and size distribution of secondary
138 species including organic aerosol (OA), sulfate, nitrate, ammonium and chloride, were measured by a
139 high-resolution time-of-flight aerosol mass spectrometer (HR-ToF-AMS, Aerodyne Research, Inc.). The
140 evolution of several volatile organic (VOCs) species were measured continually tracked by a proton
141 transfer reaction mass spectrometer (PTR-MS, Ionicon HSL experiments). Meanwhile, VOCs in the
142 chamber were also sampled by canisters every 1 hour during each experiment and analyzed by GC-
143 MS/FID system (Wang et al., 2015). Hydroxyl radical (OH) levels in the chamber were inferred from
144 the measured concentration ratios of toluene to benzene in this study (Yuan et al., 2013). Dedicated gas
145 monitors, including the SO₂, NO_x, CO, CO₂ and O₃ monitors (Thermo), were utilized, and calibrated each
146 experiment day. Zero airflow was connected to the chamber during experiment to make up the sampling
147 airflow.

148 **3 Results**

149 **3.1 Simulation of SOA formation from gasoline exhausts.** The temporal evolution of gas- and particle-
150 phase species during the chamber experiment was examined and is illustrated in Figure 2. The vehicle
151 exhaust was diluted for about 20 times in CVS and additional 15 times in the chamber. The initial



152 concentration of NO_x , benzene and toluene in the chamber were 163 ppb, 5.6 ppb and 16.8 ppb,
153 respectively, corresponding to the severe urban haze condition in the megacities (Guo et al., 2014). After
154 the chamber was exposed to the sunlight, 99% of NO was converted to NO_2 within the first 10 min due
155 to fast photolysis of H_2O_2 inside chamber. Then, the concentration of O_3 increased rapidly to approximate
156 400 ppb after 1 h exposure, and gradually decreased later in this experiment (Fig.2a).

157 Over the entire experiment, benzene and toluene experienced gentle decay in the concentrations,
158 but with different decay coefficients (Fig. 2b). Aerosol evolution is always characterized by a
159 photochemical-age-based parameterization method in ambient measurements as well as chamber
160 experiments (Hu et al., 2013;de Gouw et al., 2005;Peng et al., 2016a). Therefore, in order compare our
161 SOA production in different experiments (in which solar flux were different from each other), OH
162 exposures are calculated based on the ratios of benzene and toluene concentrations, which react at
163 different rates with OH radical (de Gouw et al., 2005). Besides, assuming that the OH concentration is
164 $1.6 \times 10^6 \text{ cm}^{-3}$, photochemical age is estimated to compare our results with the previous ambient
165 measurements (Hu et al., 2013;Peng et al., 2016a).

166 New particle formation occurred inside the chamber within 10 min of exposure to the sunlight (Fig.
167 2c). These newly formed particles performed as seeds for the further formation of secondary species. A
168 large quantity of secondary aerosols was then formed in the chamber, leading to the fast growth in the
169 diameter of these particles to approximately 70 nm after 3h aging. The measurement of the particle
170 compositions by a High time resolution ToF Aerosol Mass Spectrometer (AMS) reveals that the largest
171 mass fraction of secondary aerosols in the chamber was SOA (approximately 96%, Fig. S2), indicating
172 the critical role of the SOA for the secondary aerosol formation from gasoline exhausts. Because of the
173 low aerosol loading (initially lower than $2 \mu\text{g m}^{-3}$) and low relative humidity (40 - 50%) inside the
174 chamber, heterogeneous reactions and aqueous phase processing were not important for the formation of
175 SOA in this study (Zhang et al., 2015). Furthermore, the O:C ratio of SOA formed in the chamber stayed
176 stable around 0.4 over the entire experiment, indicating that condensed phase reactions, i.e., aqueous or
177 heterogeneous reactions, which produce high oxidized oligomers, was not significant in the chamber
178 experiments in this study. These SOA, therefore, were likely formed via condensation of less volatile
179 products oxidized through gas phase reactions of VOCs precursors with limited multigenerational
180 chemistry (Robinson et al., 2007;Jimenez et al., 2009;Jathar et al., 2014). The AMS spectrum profile of
181 gasoline SOA obtained in this study is highly correlated with the ambient SV-OOA in Beijing ($R^2=0.99$,



182 Fig. S3), further confirming the important contribution of gasoline emission on ambient $PM_{2.5}$.

183 SOA production per fuel consumption/mileage is calculated on the basis of SOA formation inside
184 the chamber, dilution factors both in the CVS and inside the chamber, and fuel consumption/mileage for
185 our working cycle. SOA mass concentration inside the chamber is corrected according to the particle
186 wall loss curve (Fig. S4) as well as the dilution effect for both particles and gas precursors (Fig. S5).
187 SOA production at the end of this experiment is calculated to be $80 \text{ mg kg-fuel}^{-1}$, or 6.7 mg km^{-1} (Fig.
188 2d). These values are 5 times higher than the emission factors of primary organic aerosols (POA) for the
189 same vehicle at the same cycle.

190 **3.2 Fuel impacts on SOA production.** High-aromatic content gasoline leads to appreciably large
191 enhancement on SOA production from both vehicle and engine experiments. As illustrated in Figure 3a,
192 the final SOA production from gasoline vehicle exhaust ranged from $30 \text{ mg kg-fuel}^{-1}$ to $98 \text{ mg kg-fuel}^{-1}$
193 at the end of each experiment, comparable to the results from cold start experiments in previous studies
194 (Gordon et al., 2014a;Jathar et al., 2014). Experiments using F3 fuel (with 36.7 % v/v aromatic content)
195 exhibit the highest SOA production factors, followed by F1 fuel (with 29.8 % v/v aromatics content) and
196 F2 fuel (with 28.5 % v/v aromatics content), successively. The average SOA production at after 12
197 photochemical-hours using F3 fuel was $76 \text{ mg kg-fuel}^{-1}$, equivalent to 3 times of that using F2 fuel, which
198 has similar parameters with F3 fuel except the aromatic content. In addition, we observe noticeably large
199 amount of the SOA formation in the first few photochemical hours in all experiments. The production
200 rate of SOA can be as high as $5 - 13 \text{ mg kg}^{-1} \text{ h}^{-1}$, indicating the existence of some semi-volatile species
201 that could partition to particle phase after first generation oxidation (Keyte et al., 2013;Robinson et al.,
202 2007).

203 SOA formation experiments from an experimental PFI engine exhaust were conducted under high
204 oxidizing condition to obtain the SOA formation potential. As illustrated in Figure 3b, most of the SOA
205 were formed within the first half an hour of each engine experiment and very little increase was observed
206 over the following hours. The SOA formation potential from the engine exhaust using F3 fuel is 3.3 g
207 kg-fuel^{-1} at this condition, equivalent to 5.6 folders of that using F2 fuel, which is $0.59 \text{ g kg-fuel}^{-1}$ on
208 average. The high emission of experimental PFI engine suggests that our engine exhaust experiment can
209 represent the SOA production from gasoline vehicles with low treatment technics. Therefore, our results
210 with two different experimental sets demonstrate the applicability of the enhancement of SOA formation
211 using high-aromatic fuel, using either high or low after treatment technology, at either representative



212 cycle condition or steady-state operating condition.

213 Though good reproducibility is found for SOA production using either F2 or F3 fuels, there are
214 inevitably several biases in the chamber simulation approach. For example, the SOA production in both
215 vehicle and engine experiments might be underestimated due to loss of semi-volatile vapors to the
216 chamber wall as well as the condensation of low organic vapor onto the particles that already lost on the
217 chamber wall (Zhang et al., 2014). Also, the SOA production in engine experiments could be
218 overestimated because the high concentration in the chamber might drive the gas-particle partitioning of
219 the semi-volatile components into particle phase (Robinson et al., 2007). Nevertheless, the relative
220 enhancement factor of SOA for different fuels is not largely influenced by these biases.

221 **3.3 Aromatic emission and SOA production.** To reveal the reason of this large amplification on SOA
222 production owing to fuel constitution, gasoline PM and VOC emissions using F2 and F3 fuels were
223 investigated and their emission factors (EFs) are illustrated in Figure 4. Huge differences in EFs among
224 different gas- and particle-phase species were observed. For example, EFs of PM in both number and
225 mass concentration using F3 fuel were only 20% larger than those using F2 fuel, consistent with previous
226 studies (Administration.). Similar results are also obtained for most of the alkane VOCs as well as NO.
227 On the contrary, the EFs for three types of species exhibit marked enhancement using high-aromatic
228 gasoline fuel, i.e., SOA, aromatic VOCs and particle-phase Polycyclic Aromatic Hydrocarbons (PAHs).
229 The EFs of each aromatic VOCs from the exhaust experimented an increase by 0.2 to 9.5 using high-
230 aromatic gasoline fuel, with an enhancement factor for total aromatic VOCs of 3.3 and 2.7 in vehicle and
231 engine experiments, respectively (Fig. 4). Coincidentally, the total particle-phase PAHs amplified for 1.8
232 times using high-aromatic gasoline fuel, with the amplification factor of each PAH species varied from
233 1.1 to 2.2. This reveals that the high-aromatic content fuel will favour the emission of all aromatic species
234 from one cycle to seven cycles, including some aromatic semi-volatile organic components (SVOC).

235 There are two main routes of aromatic components into the exhaust, which are fuel aromatic
236 survival and combustion-derived aromatics. Ethylene and acetylene are the key species for the
237 combustion-derived aromatics. High concentration of ethylene and acetylene will accelerate the
238 acetylene addition reaction, which will generate light aromatic VOC as well as PAHs in the
239 engine (Frenklach, 2002; Wang and Frenklach, 1997). In this study, when the high-aromatic fuel was used,
240 the concentrations of ethylene and acetylene from GDI engine before the three-way catalyst met an
241 enhancement by a factor of 3.3 and 2.7, respectively (Fig. 4), suggesting that more acetylene and ethylene



242 were formed from the dissociation of fuel aromatic contents.

243 SOA production ($\Delta O A_{prediction}$) from aromatic VOCs in the exhaust by multiplying the mass loss
244 of each aromatic VOC precursor (Δi) by its SOA yield, Y_i (Donahue et al., 2006):

$$245 \quad \Delta O A_{predicted} = \sum_i (\Delta_i \times Y_i) \quad (1)$$

246 The SOA precursors here include benzene, toluene, C8-aromatics, C9-aromatics and styrene. SOA
247 formation from C10-aromatics, alkenes and alkanes is found to be neglectable and are not taken account
248 in SOA prediction in this study. The yields of VOC $_i$ under high NO $_x$ condition are used (Platt et al.,
249 2013;Ng et al., 2007), due to the low initial VOCs/NO $_x$ ratios which ranged from 0.5 to 1.0.

250 Figure 5 exhibits the two typical experiments with observed and predicted SOA concentration as
251 a function of photochemical age using F2 and F3 fuels, respectively. The predicted SOA in the end of
252 the two experiments accounts for 46% and 30% of the observed SOA formation with toluene and C9-
253 aromatics to be the largest contributors, consistent with the previous results (Gordon et al., 2014a;Platt
254 et al., 2013;Nordin et al., 2013). Predicted SOA concentration using F3 fuel is about 90% higher than
255 that using F2 fuel, suggesting the import role of single-ring aromatic VOCs on the enhancement of SOA
256 formation using high-aromatic fuel. However, more than 50 % of the SOA concentration cannot be
257 explained by gas-phase oxidation of these single-ring aromatic VOCs. This value is even large (up to
258 80%) in the first few photochemical hours in both experiments. In addition, much larger percentage of
259 SOA using F3 fuel cannot be explained by the single-ring aromatic VOCs. This suggests the existence
260 of some unspeicated organic vapors, most likely semi-volatile species, which are considered to have both
261 large emission factor from vehicles and high SOA yield and might partition to particle phase after first
262 generation oxidation (Chan et al., 2009;Liu et al., 2015b;Robinson et al., 2007;Jathar et al., 2014). Two-
263 ring and three-ring gas phase PAHs, e.g., naphthalene and phenanthrene, which have been proved to have
264 higher EFs using high-aromatic fuel (Chan et al., 2009), are a majority of these unspeicated organic
265 vapors and may play a crucial role for the enhancement of SOA production using high-aromatic fuel.

266 **4 Discussion**

267 Our results exhibit the critical impact of gasoline aromatics on urban SOA formation. We observed
268 an amplification factor of 3-6 on SOA formation using high-aromatic gasoline, which is mainly caused
269 by the high emission of one-ring aromatic VOC as well as SVOC such low-molecular PAHs. This
270 enhancement of SOA formation, meanwhile, is found not only using a new vehicle with new after



271 treatment technology at a representative cycle condition, but also using experimental engine with not
272 well-performed after treatment at steady-state operating condition, suggesting the extensive applicability.

273 Moreover, photo-oxidation of aromatics leads to significant production of small dicarbonyls, i.e.,
274 glyoxal and methylglyoxal, which have high SOA yield via aqueous reactions (Zhang et al., 2015). If
275 this aqueous SOA pathway is taken account, the influence of fuel on SOA formation will be much more
276 remarkable. More work is needed to evaluate the aqueous pathway of SOA formation from gasoline
277 exhaust.

278 Currently, aromatic content in gasoline fuel is increasing continuous in China, where more
279 stringent standard on gasoline sulfur content are undertaking and the oil refining procedure are changing
280 to meet the new standard. For example, we found the average aromatic content for gasoline fuel in the
281 market meeting Beijing III, IV and V standards were 23.4%, 28.5% and 36.3%, respectively. Hence,
282 the enhancement in SOA formation exerted by the increase of aromatic content in gasoline fuel from 29%
283 to 37 % in this study can well represent the extra SOA formation due to the gasoline standard change in
284 Beijing. Neglect of this side effect of fuel standard change may partially offset the tremendous endeavors
285 on vehicle emission control by the local government. From another perspective, our findings provide a
286 new direction in controlling air pollution from vehicles, which is to decrease the aromatic content in the
287 gasoline fuel. This may request more hydrogenation catalysis instead of catalytic reforming in the
288 petroleum refining procedure. Compared with the vehicle restriction regulation that met the shrill
289 opposition voice from the society and the elimination of polluted vehicles that brought large amount of
290 expenses, this direction might be more acceptable, efficient and economical. Additionally, current
291 vehicle emission evaluation system, which mainly measures the emissions of PM, THC, NO_x and CO,
292 will fail to tell the consequences of using the high-aromatic gasoline fuel, as these species do not increase
293 much when high-aromatic fuel is using (Fig. 4). Aromatic VOCs, especially the SVOC, should be
294 considered in future vehicle emission evaluation.

295 Furthermore, this influence of gasoline aromatic content on air quality is not only adoptable in
296 China. Strikingly, the current standard on gasoline aromatic content are not stringent enough in most of
297 the countries and regions in the world, where fuel standards with very high maximum gasoline aromatic
298 content (ranging from 35% to 42% in different countries) are implemented, even including some
299 developed countries and regions, i.e., Europe, Japan, Australia. Our findings highlight the necessity of a
300 more stringent regulation on gasoline aromatic content in the next renewal of the gasoline standard.



301 **Acknowledgement**

302 This work was supported by the National Basic Research Program of China (973 Program)
303 (2013CB228503, 2013CB228502); National Natural Science Foundation of China (91544214, 51636003,
304 41421064); the Strategic Priority Research Program of Chinese Academy of Sciences (XDB05010500);
305 China Postdoctoral Science Foundation (2015M580929).

306

307 **References**

308 Bahreini, R., Middlebrook, A. M., de Gouw, J. A., Warneke, C., Trainer, M., Brock, C. A., Stark, H.,
309 Brown, S. S., Dube, W. P., Gilman, J. B., Hall, K., Holloway, J. S., Kuster, W. C., Perring, A. E.,
310 Prevot, A. S. H., Schwarz, J. P., Spackman, J. R., Szidat, S., Wagner, N. L., Weber, R. J., Zotter, P.,
311 and Parrish, D. D.: Gasoline emissions dominate over diesel in formation of secondary organic
312 aerosol mass, *Geophys. Res. Lett.*, 39, doi:10.1029/2011gl050718, 2012.

313 Chan, A. W. H., Kautzman, K. E., Chhabra, P. S., Surratt, J. D., Chan, M. N., Crounse, J. D., Kurten, A.,
314 Wennberg, P. O., Flagan, R. C., and Seinfeld, J. H.: Secondary organic aerosol formation from
315 photooxidation of naphthalene and alkylnaphthalenes: implications for oxidation of intermediate
316 volatility organic compounds (IVOCs), *Atmos. Chem. Phys.*, 9, 3049-3060, doi:10.5194/acp-9-3049-
317 2009, 2009.

318 de Gouw, J. A., Middlebrook, A. M., Warneke, C., Goldan, P. D., Kuster, W. C., Roberts, J. M.,
319 Fehsenfeld, F. C., Worsnop, D. R., Canagaratna, M. R., Pszenny, A. A. P., Keene, W. C., Marchewka,
320 M., Bertman, S. B., and Bates, T. S.: Budget of organic carbon in a polluted atmosphere: Results
321 from the New England Air Quality Study in 2002, *J. Geophys. Res.-Atmos.*, 110,
322 doi:10.1029/2004jd005623, 2005.

323 Donahue, N. M., Robinson, A. L., Stanier, C. O., and Pandis, S. N.: Coupled partitioning, dilution, and
324 chemical aging of semivolatile organics, *Environ. Sci. Technol.*, 40, 2635-2643,
325 doi:10.1021/es052297c, 2006.

326 Du, Z., Hu, M., Peng, J., Guo, S., Zheng, R., Zheng, J., Shang, D., Qin, Y., Niu, H., Li, M., Yang, Y.,
327 Lu, S., Wu, Y., Shao, M., and Shuai, S.: The Potential of Secondary Aerosol Formation from Chinese
328 Gasoline Engine Exhaust. *J. Environ. Sci.*, in press, 2017.

329 Energy Information Administration U.S.: October 2014 Monthly Energy Review, DOE/EIA-
330 0035(2014/10), <http://www.eia.gov/totalenergy/data/monthly/pdf/mer.pdf>, 2014.



- 331 Environmental Protection Agency U.S.: Assessing the Effect of Five Gasoline Properties on Exhaust
332 Emissions from Light-Duty Vehicles Certified to Tier 2 Standards: Analysis of Data from EPA's
333 Phase 3., EPA-420-R-13-002:232-233, 2013.
- 334 Frenklach, M.: Reaction mechanism of soot formation in flames, *Phys. Chem. Chem. Phys.*, 4, 2028-
335 2037, doi:10.1039/b110045a, 2002.
- 336 Gordon, T. D., Presto, A. A., May, A. A., Nguyen, N. T., Lipsky, E. M., Donahue, N. M., Gutierrez, A.,
337 Zhang, M., Maddox, C., Rieger, P., Chattopadhyay, S., Maldonado, H., Maricq, M. M., and Robinson,
338 A. L.: Secondary organic aerosol formation exceeds primary particulate matter emissions for light-
339 duty gasoline vehicles, *Atmos. Chem. and Phys.*, 14, 4661-4678, doi:10.5194/acp-14-4661-2014,
340 2014a.
- 341 Gordon, T. D., Presto, A. A., Nguyen, N. T., Robertson, W. H., Na, K., Sahay, K. N., Zhang, M., Maddox,
342 C., Rieger, P., Chattopadhyay, S., Maldonado, H., Maricq, M. M., and Robinson, A. L.: Secondary
343 organic aerosol production from diesel vehicle exhaust: impact of aftertreatment, fuel chemistry and
344 driving cycle, *Atmos. Chem. Phys.*, 14, 4643-4659, doi:10.5194/acp-14-4643-2014, 2014b.
- 345 Guo, S., Hu, M., Zamora, M. L., Peng, J. F., Shang, D. J., Zheng, J., Du, Z. F., Wu, Z., Shao, M., Zeng,
346 L. M., Molina, M. J., and Zhang, R. Y.: Elucidating severe urban haze formation in China, *P. Natl.*
347 *Acad. Sci. U.S.A.*, 111, 17373-17378, doi:10.1073/pnas.1419604111, 2014.
- 348 Hu, W. W., Hu, M., Yuan, B., Jimenez, J. L., Tang, Q., Peng, J. F., Hu, W., Shao, M., Wang, M., Zeng,
349 L. M., Wu, Y. S., Gong, Z. H., Huang, X. F., and He, L. Y.: Insights on organic aerosol aging and
350 the influence of coal combustion at a regional receptor site of central eastern China, *Atmos. Chem.*
351 *Phys.*, 13, 10095-10112, doi:10.5194/acp-13-10095-2013, 2013.
- 352 Huang, R.-J., Zhang, Y., Bozzetti, C., Ho, K.-F., Cao, J.-J., Han, Y., Daellenbach, K. R., Slowik, J. G.,
353 Platt, S. M., Canonaco, F., Zotter, P., Wolf, R., Pieber, S. M., Bruns, E. A., Crippa, M., Ciarelli, G.,
354 Piazzalunga, A., Schwikowski, M., Abbaszade, G., Schnelle-Kreis, J., Zimmermann, R., An, Z.,
355 Szidat, S., Baltensperger, U., Haddad, I. E., and Prévôt, A. S. H.: High secondary aerosol contribution
356 to particulate pollution during haze events in China, *Nature*, doi:10.1038/nature13774, 2014.
- 357 Jathar, S. H., Miracolo, M. A., Tkacik, D. S., Donahue, N. M., Adams, P. J., and Robinson, A. L.:
358 Secondary Organic Aerosol Formation from Photo-Oxidation of Unburned Fuel: Experimental
359 Results and Implications for Aerosol Formation from Combustion Emissions, *Environ. Sci. Technol.*,
360 47, 12886-12893, doi:10.1021/es403445q, 2013.



- 361 Jathar, S. H., Gordon, T. D., Hennigan, C. J., Pye, H. O., Pouliot, G., Adams, P. J., Donahue, N. M., and
362 Robinson, A. L.: Unspeciated organic emissions from combustion sources and their influence on the
363 secondary organic aerosol budget in the United States, *P. Natl. Acad. Sci. U.S.A.*, 111, 10473-10478,
364 doi:10.1073/pnas.1323740111, 2014.
- 365 Jimenez, J. L., Canagaratna, M. R., Donahue, N. M., Prevot, A. S. H., Zhang, Q., Kroll, J. H., DeCarlo,
366 P. F., Allan, J. D., Coe, H., Ng, N. L., Aiken, A. C., Docherty, K. S., Ulbrich, I. M., Grieshop, A. P.,
367 Robinson, A. L., Duplissy, J., Smith, J. D., Wilson, K. R., Lanz, V. A., Hueglin, C., Sun, Y. L., Tian,
368 J., Laaksonen, A., Raatikainen, T., Rautiainen, J., Vaattovaara, P., Ehn, M., Kulmala, M., Tomlinson,
369 J. M., Collins, D. R., Cubison, M. J., Dunlea, J., Huffman, J. A., Onasch, T. B., Alfarra, M. R.,
370 Williams, P. I., Bower, K., Kondo, Y., Schneider, J., Drewnick, F., Borrmann, S., Weimer, S.,
371 Demerjian, K., Salcedo, D., Cottrell, L., Griffin, R., Takami, A., Miyoshi, T., Hatakeyama, S.,
372 Shimono, A., Sun, J. Y., Zhang, Y. M., Dzepina, K., Kimmel, J. R., Sueper, D., Jayne, J. T., Herndon,
373 S. C., Trimborn, A. M., Williams, L. R., Wood, E. C., Middlebrook, A. M., Kolb, C. E., Baltensperger,
374 U., and Worsnop, D. R.: Evolution of Organic Aerosols in the Atmosphere, *Science*, 326, 1525-1529,
375 doi:10.1126/science.1180353, 2009.
- 376 Karavalakis, G., Short, D., Vu, D., Russell, R., Hajbabaie, M., Asa-Awuku, A., and Durbin, T. D.:
377 Evaluating the Effects of Aromatics Content in Gasoline on Gaseous and Particulate Matter
378 Emissions from SI-PFI and SIDI Vehicles, *Environ. Sci. Technol.*, 49, 7021-7031,
379 doi:10.1021/es5061726, 2015.
- 380 Kelly, F. J., and Zhu, T.: Transport solutions for cleaner air, *Science*, 352, 934-936,
381 doi:10.1126/science.aaf3420, 2016.
- 382 Keyte, I. J., Harrison, R. M., and Lammel, G.: Chemical reactivity and long-range transport potential of
383 polycyclic aromatic hydrocarbons - a review, *Chem Soc Rev*, 42, 9333-9391, 10.1039/c3cs60147a,
384 2013.
- 385 Kumar, P., Morawska, L., Birmili, W., Paasonen, P., Hu, M., Kulmala, M., Harrison, R. M., Norford, L.,
386 and Britter, R.: Ultrafine particles in cities, *Environ. Int.*, 66, 1-10, doi:10.1016/j.envint.2014.01.013,
387 2014.
- 388 Liu, S., Aiken, A. C., Gorkowski, K., Dubey, M. K., Cappa, C. D., Williams, L. R., Herndon, S. C.,
389 Massoli, P., Fortner, E. C., Chhabra, P. S., Brooks, W. A., Onasch, T. B., Jayne, J. T., Worsnop, D.
390 R., China, S., Sharma, N., Mazzoleni, C., Xu, L., Ng, N. L., Liu, D., Allan, J. D., Lee, J. D., Fleming,



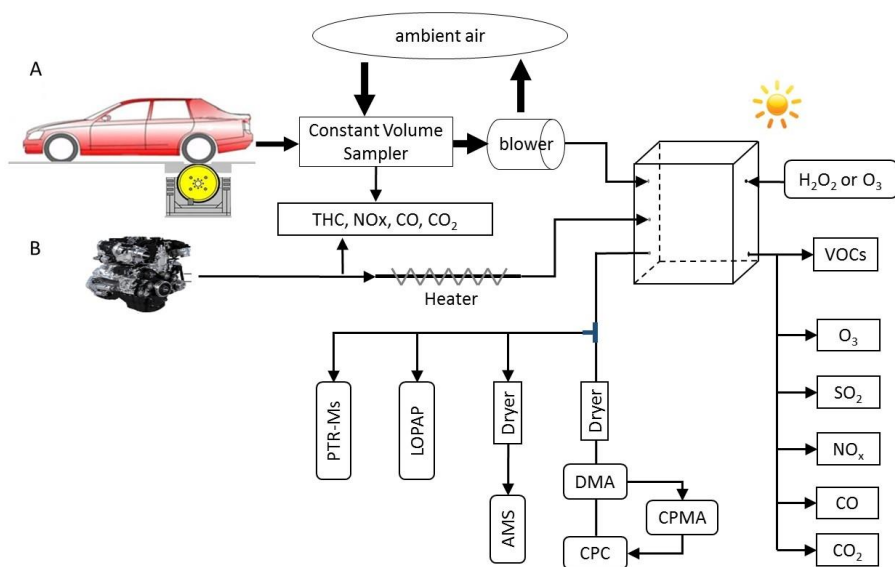
- 391 Z. L., Mohr, C., Zotter, P., Szidat, S., and Prevot, A. S. H.: Enhanced light absorption by mixed
392 source black and brown carbon particles in UK winter, *Nat. Commun.*, 6, doi:10.1038/Ncomms9435,
393 2015a.
- 394 Liu, T., Wang, X., Deng, W., Hu, Q., Ding, X., Zhang, Y., He, Q., Zhang, Z., Lu, S., Bi, X., Chen, J.,
395 and Yu, J.: Secondary organic aerosol formation from photochemical aging of light-duty gasoline
396 vehicle exhausts in a smog chamber, *Atmos. Chem. Phys.*, 15, 9049-9062, doi:10.5194/acp-15-9049-
397 2015, 2015b.
- 398 NBSC National Bureau of Statistics of China: China Statistical Yearbook, China Statistics Press, 2015.
- 399 Ng, N. L., Kroll, J. H., Chan, A. W. H., Chhabra, P. S., Flagan, R. C., and Seinfeld, J. H.: Secondary
400 organic aerosol formation from m-xylene, toluene, and benzene, *Atmos. Chem. Phys.*, 7, 3909-3922,
401 2007.
- 402 Nordin, E. Z., Eriksson, A. C., Roldin, P., Nilsson, P. T., Carlsson, J. E., Kajos, M. K., Hellén, H.,
403 Wittbom, C., Rissler, J., Löndahl, J., Swietlicki, E., Svenningsson, B., Bohgard, M., Kulmala, M.,
404 Hallquist, M., and Pagels, J. H.: Secondary organic aerosol formation from idling gasoline passenger
405 vehicle emissions investigated in a smog chamber, *Atmos. Chem. Phys.*, 13, 6101-6116,
406 doi:10.5194/acp-13-6101-2013, 2013.
- 407 Parrish, D. D., and Zhu, T.: Clean Air for Megacities, *Science*, 326, 674-675,
408 doi:10.1126/science.1176064, 2009.
- 409 Peng, J. F., Hu, M., Gong, Z. H., Tian, X. D., Wang, M., Zheng, J., Guo, Q. F., Cao, W., Lv, W., Hu, W.
410 W., Wu, Z. J., and Guo, S.: Evolution of secondary inorganic and organic aerosols during transport:
411 A case study at a regional receptor site, *Environ. Pollut.*, 218, 794-803,
412 doi:10.1016/j.envpol.2016.08.003, 2016a.
- 413 Peng, J. F., Hu, M., Guo, S., Du, Z. F., Zheng, J., Shang, D. J., Zamora, M. L., Zeng, L. M., Shao, M.,
414 Wu, Y. S., Zheng, J., Wang, Y., Glen, C. R., Collins, D. R., Molina, M. J., and Zhang, R. Y.: Markedly
415 enhanced absorption and direct radiative forcing of black carbon under polluted urban environments,
416 *P. Natl. Acad. Sci. U.S.A.*, 113, 4266-4271, doi:10.1073/pnas.1602310113, 2016b.
- 417 Platt, S. M., El Haddad, I., Zardini, A. A., Clairrotte, M., Astorga, C., Wolf, R., Slowik, J. G., Temime-
418 Roussel, B., Marchand, N., Ježek, I., Drinovec, L., Močnik, G., Möhler, O., Richter, R., Barmet, P.,
419 Bianchi, F., Baltensperger, U., and Prévôt, A. S. H.: Secondary organic aerosol formation from
420 gasoline vehicle emissions in a new mobile environmental reaction chamber, *Atmos. Chem. Phys.*,



- 421 13, 9141-9158, doi:10.5194/acp-13-9141-2013, 2013.
- 422 Platt, S. M., El Haddad, I., Pieber, S. M., Huang, R. J., Zardini, A. A., Clairotte, M., Suarez-Bertoa, R.,
423 Barmet, P., Pfaffenberger, L., Wolf, R., Slowik, J. G., Fuller, S. J., Kalberer, M., Chirico, R.,
424 Dommen, J., Astorga, C., Zimmermann, R., Marchand, N., Hellebust, S., Temime-Roussel, B.,
425 Baltensperger, U., and Prevot, A. S. H.: Two-stroke scooters are a dominant source of air pollution
426 in many cities, *Nat. Commun.*, 5, doi:10.1038/Ncomms4749, 2014.
- 427 Robinson, A. L., Donahue, N. M., Shrivastava, M. K., Weitkamp, E. A., Sage, A. M., Grieshop, A. P.,
428 Lane, T. E., Pierce, J. R., and Pandis, S. N.: Rethinking Organic Aerosols: Semivolatile Emissions
429 and Photochemical Aging, *Science*, 315, 1259-1262, doi:10.1126/science.1133061, 2007.
- 430 Wang, H., and Frenklach, M.: A detailed kinetic modeling study of aromatics formation in laminar
431 premixed acetylene and ethylene flames, *Combust. Flame*, 110, 173-221, doi:10.1016/S0010-
432 2180(97)00068-0, 1997.
- 433 Wang, M., Shao, M., Chen, W., Lu, S., Liu, Y., Yuan, B., Zhang, Q., Zhang, Q., Chang, C. C., Wang,
434 B., Zeng, L., Hu, M., Yang, Y., and Li, Y.: Trends of non-methane hydrocarbons (NMHC) emissions
435 in Beijing during 2002-2013, *Atmos. Chem. Phys.*, 15, 1489-1502, 2015.
- 436 Yinhui, W., Rong, Z., Yanhong, Q., Jianfei, P., Mengren, L., Jianrong, L., Yusheng, W., Min, H., and
437 Shijin, S.: The impact of fuel compositions on the particulate emissions of direct injection gasoline
438 engine, *Fuel*, 166, 543-552, doi:10.1016/j.fuel.2015.11.019, 2016.
- 439 Yuan, B., Hu, W. W., Shao, M., Wang, M., Chen, W. T., Lu, S. H., Zeng, L. M., and Hu, M.: VOC
440 emissions, evolutions and contributions to SOA formation at a receptor site in eastern China, *Atmos.*
441 *Chem. Phys.*, 13, 8815-8832, doi:10.5194/acp-13-8815-2013, 2013.
- 442 Zervas, E., Montagne, X., and Lahaye, J.: The influence of gasoline formulation on specific pollutant
443 emissions, *J. Air Waste. Manage.*, 49, 1304-1314, 1999.
- 444 Zhang, R., Wang, G., Guo, S., Zamora, M. L., Ying, Q., Lin, Y., Wang, W., Hu, M., and Wang, Y.:
445 Formation of urban fine particulate matter, *Chem. Rev.*, 115, 3803-3855,
446 doi:10.1021/acs.chemrev.5b00067, 2015.
- 447 Zhang, X., Cappa, C. D., Jathar, S. H., Mcvay, R. C., Ensberg, J. J., Kleeman, M. J., and Seinfeld, J. H.:
448 Influence of vapor wall loss in laboratory chambers on yields of secondary organic aerosol, *P. Natl.*
449 *Acad. Sci. U.S.A.*, 111, 5802-5807, doi:10.1073/pnas.1404727111, 2014.
- 450



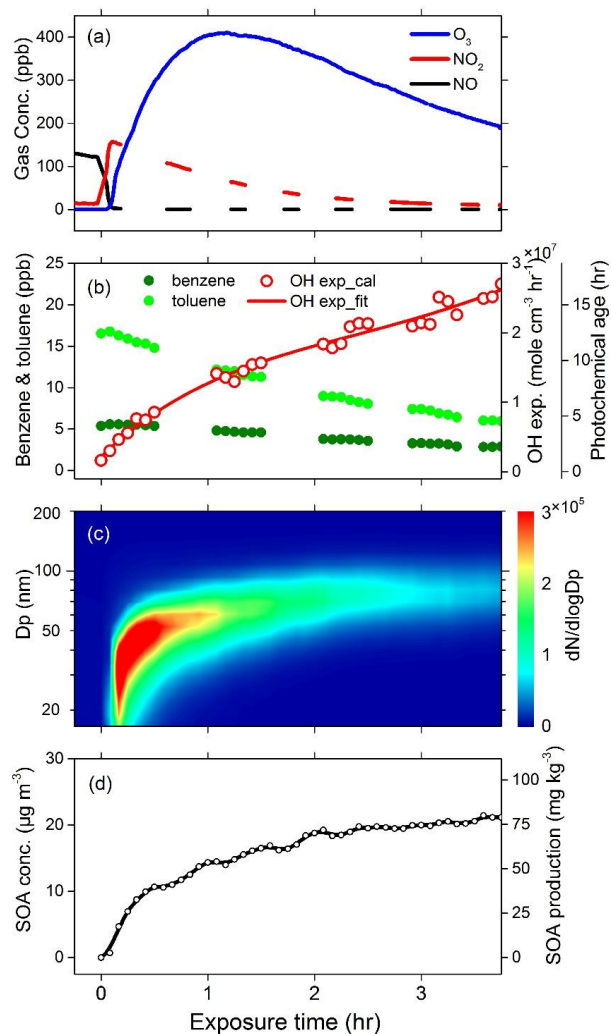
451



452

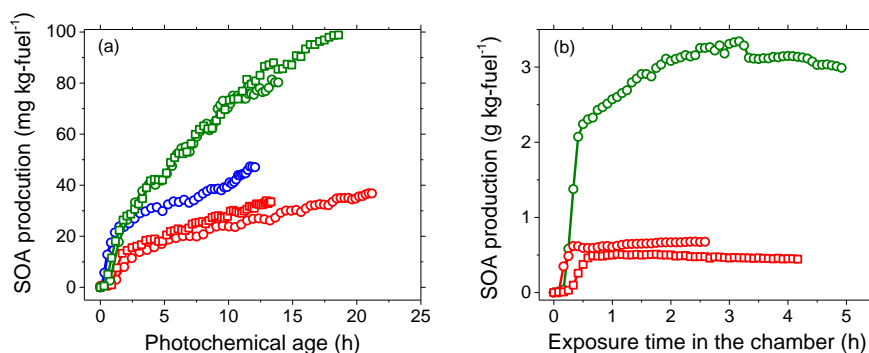
453 **Figure 1.** Schematic diagram of chamber experiments.

454



455

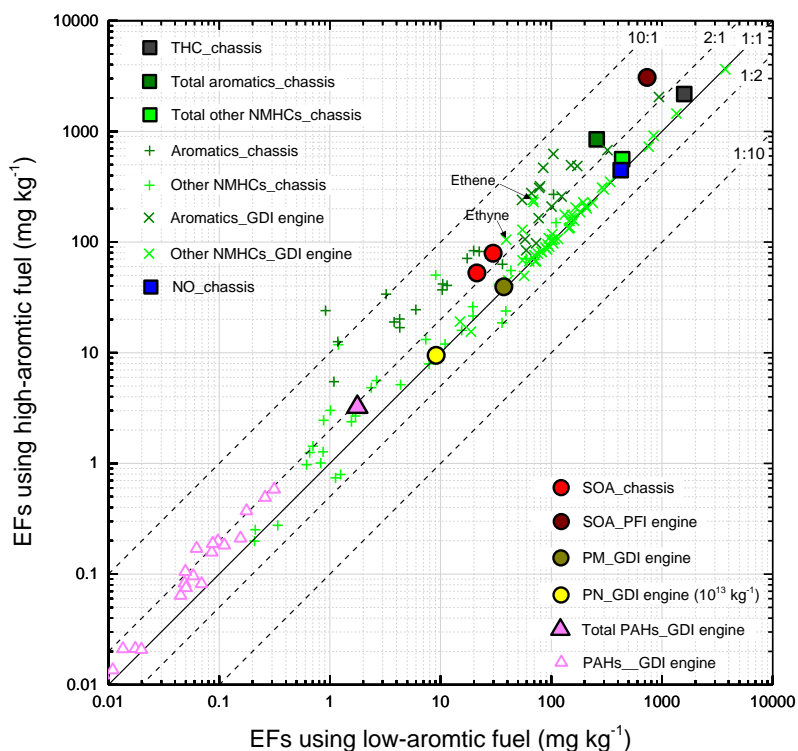
456 **Figure 2.** Evolution of gas-phase species (a, b), particle size distribution (c), and SOA concentration and
457 production (d) during a typical chamber experiment (V2). OH exposure and photochemical age are
458 calculated based on the ratios of benzene and toluene concentrations, assuming that OH concentration is
459 1.6×10^6 mole cm^{-3} . The SOA mass concentration is obtained by intergrading size distribution of particles
460 inside the chamber on the basis of measured particle density. The measured SOA mass concentration is
461 corrected according to the particle wall loss curve as well as the dilution effect for both particles and gas
462 precursors.
463



464

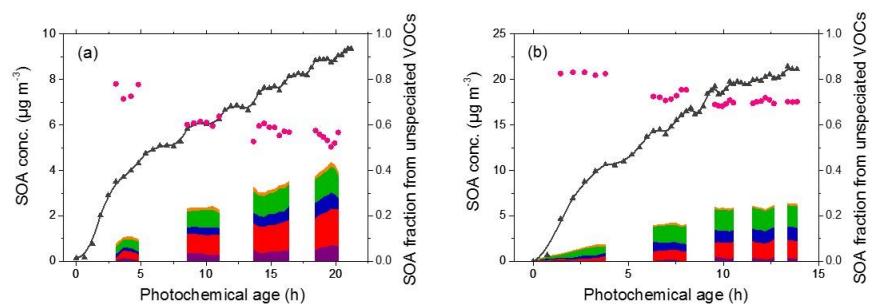
465 **Figure 3.** SOA production in the vehicle experiments as a function of photochemical age (a) and in the
466 engine exhaust experiments as a function of exposure time (b). The blue, red and green symbols represent
467 experiments using the F1, F2 and F3 fuels, respectively. The green squares, green circles, red squares,
468 red circles and blue circles (a) represent the experiments V1, V2, V3, V4 and V5 shown in Table S1,
469 respectively. The green circles, red squares and red circles (b) represent the experiments E1, E2 and E3
470 shown in Table S2, respectively.

471



472

473 **Figure 4.** Comparison of emission factors (EFs) of gas- and particle species using high-aromatic fuel (F3
474 fuel) to those using low-aromatic fuel (F2 fuel). The symbols in the figure represent as following: the red
475 circles: SOA productions after 6 and 12 photochemical hours; the wine circle: SOA production potential
476 in PFI engine experiments; the light and dark yellow circle: total particle number and mass EFs for GDI
477 engine; the hollow and solid purple triangle: EFs of each Polycyclic Aromatic Hydrocarbons (PAH) and
478 total PAHs EFs for GDI engine; the dark gray, dark green and light green solid square: EFs of total
479 hydrocarbons (THC), total aromatics and total other non-methane hydrocarbons (NMHCs) in the vehicle
480 experiments, respectively; dark green and light green crosses: EFs of aromatics and other NMHCs
481 species, respectively; blue solid square: EF of NO. The black line denotes that the ratio of EFs using
482 aromatic-rich fuel over aromatic-poor fuel is 1:1, and dashed lines stand for the ratios of 10:1, 2:1, 1:2,
483 and 1:10, respectively. Note that the PAHs and VOCs data for the GDI engine were measured before the
484 three-way Catalyst (TWC).



485

486 **Figure 5.** Observed and predicted SOA concentration, and SOA fraction from unspeciated VOCs as a
487 function of photochemical age in typical chamber experiments using F2 (a) and F3 (b) fuels. Black line
488 and triangles represent the corrected SOA concentrations in the chamber experiments. The purple, red,
489 blue, green and yellow areas represent the predicted SOA from the oxidation of benzene, toluene, C8-
490 aromatics, C9-aromatics and styrene, respectively. The pink circles represent the SOA fractions that
491 cannot be predicted by the one-ring aromatic VOC precursors.

492

493